Supporting information

How thermally stable are vanadium cathode Li-ion cells?

Fenghua Guo[a], Hui Zhou[a], Jonathan Miller[a], Brian J. Schultz[b], Leonardo Gobbato[b,c],

and M. Stanley Whittingham[a]*

[a] Department of Chemistry and Materials, State University of New York at Binghamton, Binghamton, New York 13902-6000, United States

[b] Dimien Inc., Buffalo, New York 14228, United States

[c] Department of Chemical and Biological Engineering, State University of New York at Buffalo, Buffalo, New York 14260-4200, United States

* Corresponding author. Email: stanwhit@gmail.com

Table S1. The C value and potential window used for electrochemical measurements for the electrodes.

Electrode	LFP	NMC811	ζ-V_2O_5	ε -$VOPO_4$
C value (mAh/g)	160	200	250	305
Potential window (V)	2.5 – 4.0	2.8 - 4.4	2.2 – 4.0	1.6 – 4.5

Table S2. Possible valance changes for the electrodes after ARC, identified from XRD data collected from ARC residue.

Electrode	LFP	NMC811	ζ-V_2O_5	ε -$VOPO_4$
Valance change	$Fe^{3+}\rightarrow Fe^{2+}$	$Ni^{4+}\rightarrow Ni^{2+}\rightarrow Ni^{0}$	$V^{5+}\rightarrow V^{4+}\rightarrow V^{2+}$	$V^{5+}\rightarrow V^{3+}$

Table S3. The temperature and heat flow intensity of maximum heat flux during DSC for four electrodes with LP30.

Electrode	LFP	NMC811	ζ-V_2O_5	ε -$VOPO_4$
Temperature ($^{\circ}C$)	265	213	262	222
Heat flow (W/g)	0.39	1.92	0.30	0.22

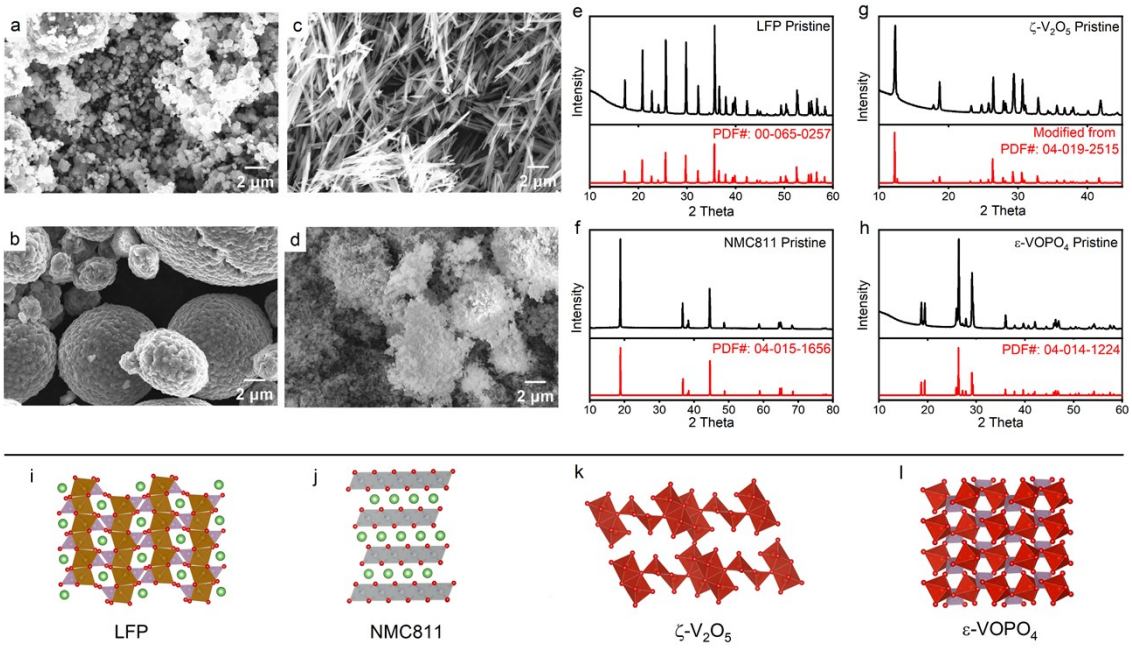

Fig. S1: SEM images and XRD patterns of the pristine particles: (a, e) LFP; (b, f) NMC811; (c, g) ζ-V_2O_5, the XRD pattern labeled in red as standard was generated with VESTA,[1] and was modified from β-$Ag_{0.4}V_2O_5$ (PDF#: 04-019-2515) by removing the Ag atoms; (d, h) ε-$VOPO_4$. Illustration of crystal structures of (i) LFP, green dots represent lithium atoms, the [PO_4] tetrahedral units were labeled in purple, and the [FeO_6] octahedral units labeled in brown; (j) NMC811, metal ions resides in the center of octahedral units with oxygen atoms at the corners, lithium atoms labeled in green locate between the layers; (k) ζ-V_2O_5, vanadium atoms reside in the distorted [VO_6] octahedral units and [VO_5] square pyramid units, while lithium ion could be accommodated in the tunnels; (l) ε-$VOPO_4$, olivine structure with distorted [VO_6] octahedral units connected by [PO_4] tetrahedral units. The crystal structure illustrations were also generated from standard patterns in (e-h) by using VESTA.[1]

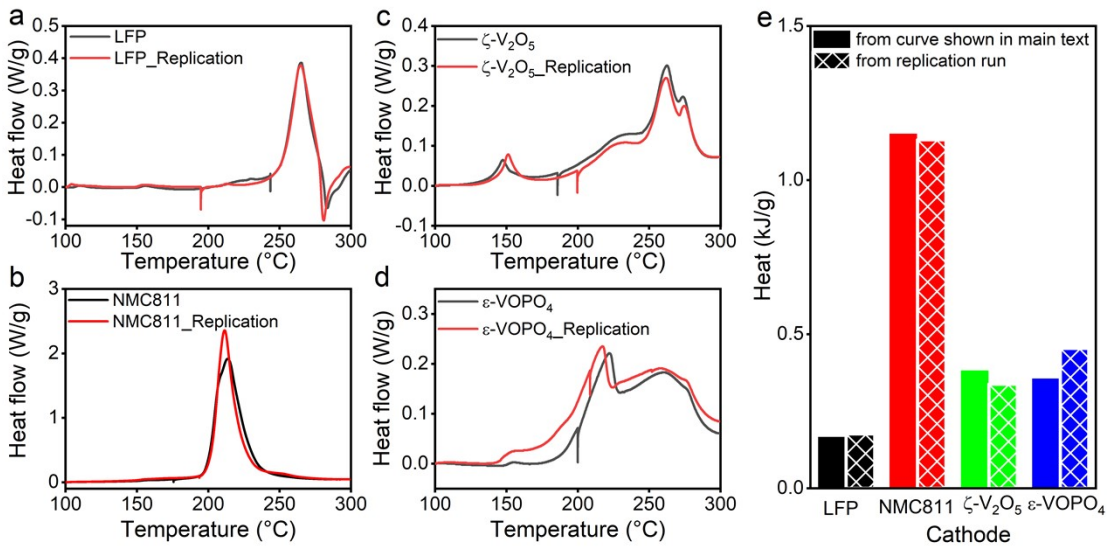

Fig. S2: Replication of DSC measurements: heat profile of (a) LFP, (b) NMC811, (c) ζ-V_2O_5, (d) ε-$VOPO_4$, and (e) integrated heat, the integrated heat shown in Fig. 2(d) was average value of the two runs shown here. The curves labeled in black in (a-d) were data shown in main text.

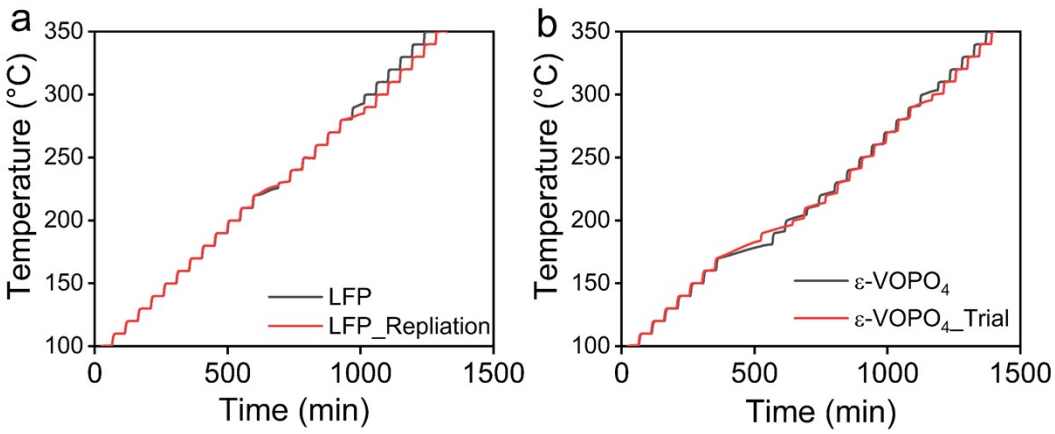

Fig. S3: The comparison between the ARC results shown in the main text and (a) a replication run of LFP, as well as (b) a trial run of ε-$VOPO_4$. The trial run was done during the optimization of test conditions for ARC, the only difference between the trial run and the run shown in main text was in the pouch cell preparation: the ratio between the mass of active material: electrolyte was 1: 4 for pouch cell shown in main text, while for trial run the ratio was 1:2.

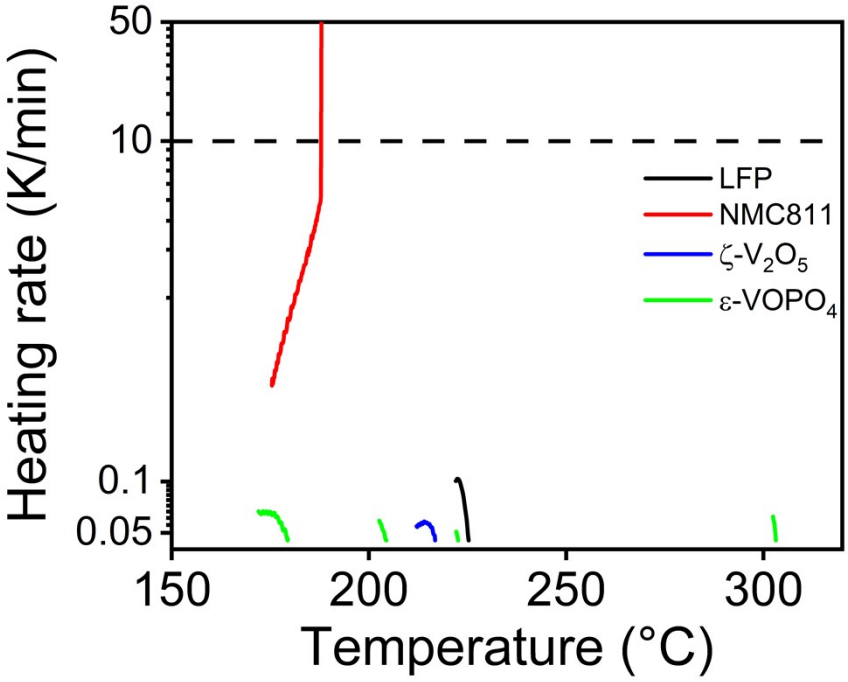

Fig. S4: Self-heating rate for each exothermic reaction region for the four charged cathodes with LP30. For NMC811, only the heating rate prior to exceeding 50 K/min was shown, after which may not be reliable as it is above the instrument's capability to keep adiabatic condition.

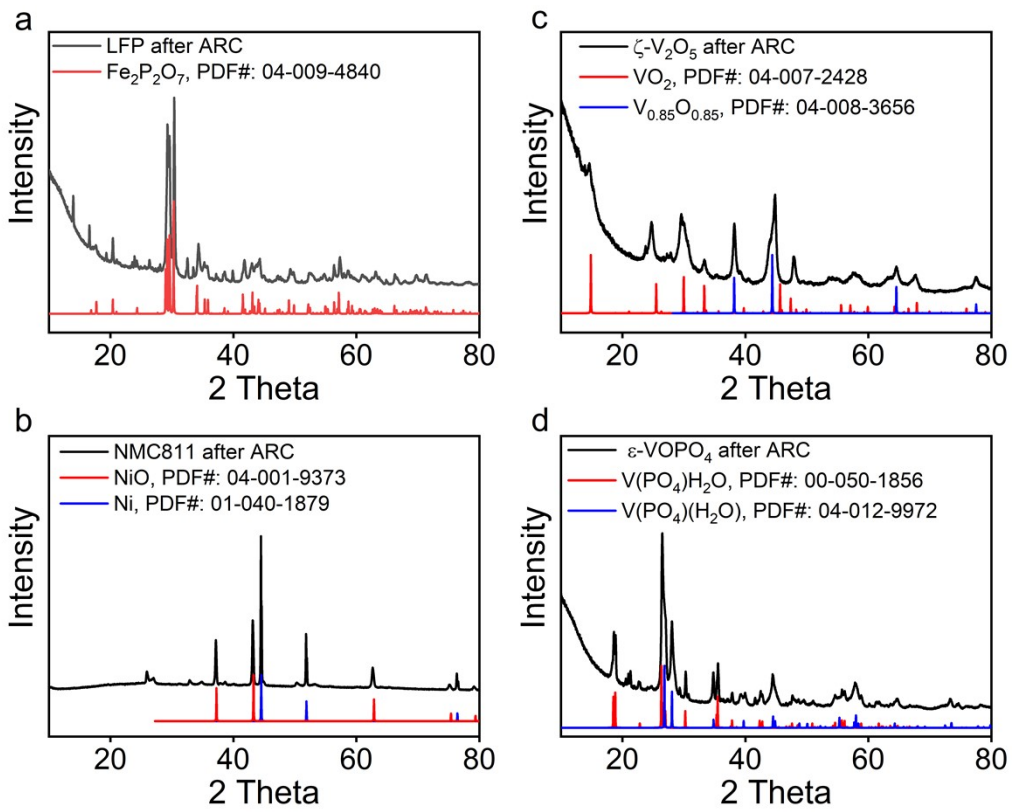

Fig. S5: XRD patterns collected on the residues collected after ARC measurement for (a) LFP, (b) NMC811, (c) ζ-V_2O_5 and (d) ε-$VOPO_4$. With the complexity of ARC residues, not all the peaks were indexed.

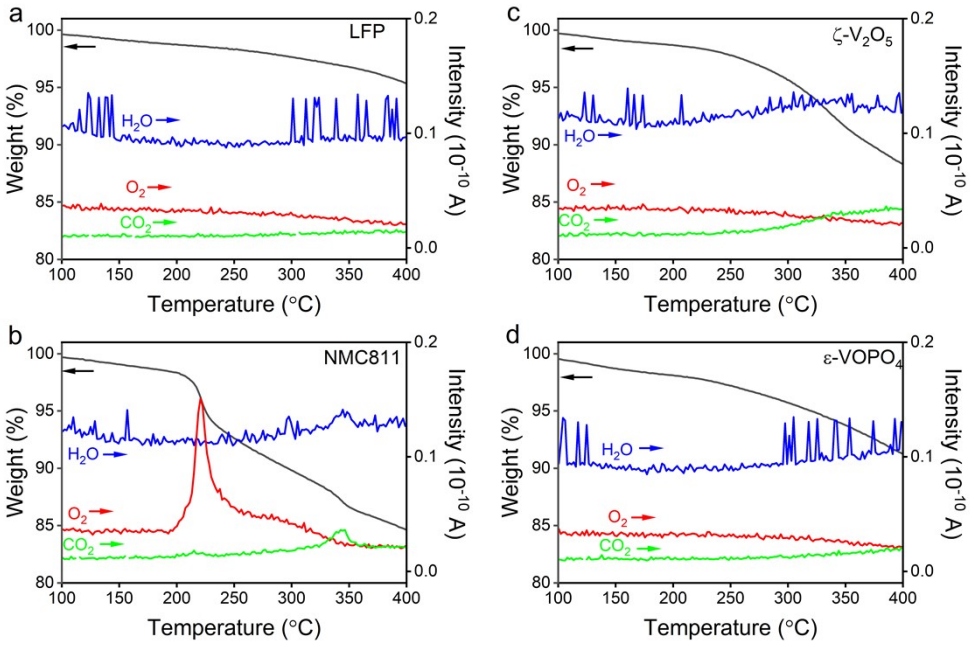

Fig. S6: TGA-MS of charged samples: (a) LFP, (b) NMC811, (c) ζ-V_2O_5 and (d) ε-$VOPO_4$.

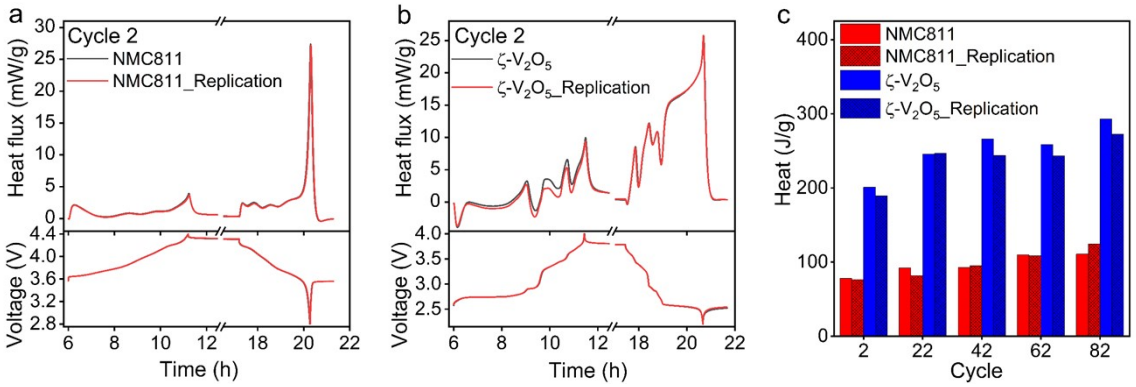

Fig. S7: To check the repeatability of in-operando heat measurements by TAM IV, the measurements with NMC811 and ζ-V_2O_5 were repeated. Comparison between the operando heat generation results shown in the main text and a replication run: (a) Cycle 2 for NMC811, (b) Cycle 2 for ζ-V_2O_5, and (c) the integrated heat at different cycles for NMC811 and ζ-V_2O_5.

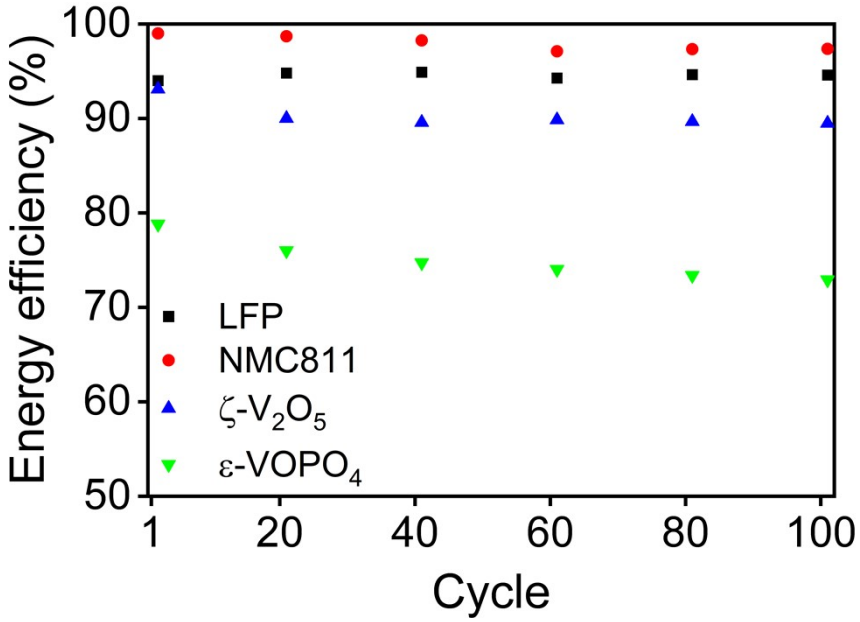

Fig. S8: Energy efficiency over cycling, calculated from integration of charge/discharge curve over capacity. The original cycling data is shown in Fig. 1(b).

Reference

1. K. Momma and F. Izumi, *Journal of applied crystallography*, 2011, **44**, 1272-1276.